Rapid earthquake rupture duration estimates from teleseismic energy rates, with application to real-time warning

Jaime Andres Convers[1] and Andrew V. Newman[1]

Received 16 August 2013; revised 9 October 2013; accepted 10 October 2013.

[1] We estimate the seismic rupture durations from global large earthquakes (moment magnitude ≥ 7.0) by characterizing changes in the radiated *P*-wave energy and by introducing the time-averaged cumulative energy rate (TACER), which approximates rupture duration based on the peak first local maximum of an earthquake's high-frequency energy measured at teleseismic broadband seismometers. TACER is particularly useful for real-time evaluations, including the identification of slow-rupturing tsunami earthquakes. In cases of long unilateral earthquake rupture and good azimuthal station distribution, the per-station behavior of TACER may identify the approximate rupture direction, rupture velocity, and length due to directivity effects. We retrospectively analyze 93 earthquakes between 2000 and 2009, and analyze another 65 earthquakes using real-time observations between January 2009 and December 2012. Real-time and retrospective results are comparable and similar to the duration expected from other studies where duration grows as the cubed-root of seismic moment. **Citation:** Convers, J. A., and A. V. Newman (2013), Rapid earthquake rupture duration estimates from teleseismic energy rates, with application to real-time warning, *Geophys. Res. Lett.*, *40*, doi:10.1002/2013GL057664.

1. Introduction

[2] The duration of dynamic rupture is an important parameter for describing earthquake source processes, most notably rupture directivity, length, and velocity of large earthquakes. Together with the total radiated seismic energy E, the rupture duration T_R is a powerful tool for rapidly discriminating between normal and slow ruptures, such as those of tsunami earthquakes [e.g., *Convers and Newman*, 2011; *Newman et al*., 2011]. Detailed estimates of earthquake rupture duration can be obtained from inverted source-time functions [e.g., *Houston*, 2001], but given its increasing importance in early determinations for tsunami warning or rapid damage assessments, it is important to accurately determine this parameter along with earthquake location, magnitudes, and focal mechanism rapidly after an earthquake occurs.

[3] Different approaches to rapidly estimating T_R have been attempted. An estimate using the time at which 90% of the radiated energy was recorded was developed by *Lomax* [2005]. Another estimate was obtained from the 25% drawdown of energy from its maximum in the envelope of a velocity seismogram between 2 and 4 Hz [*Hara*, 2007]. Both of the above methods are relatively robust, but require an arbitrary cutoff that may fail with noisy data or for complex ruptures. *Convers and Newman* [2011] use the crossover duration T_{XO}, marking the transition between near-linear cumulative energy growth and subsequent scattered energy, to estimate the termination of rupture and the point where they calculate the radiated energy. While T_{XO} works well in most cases, it requires averaging results from numerous stations and usually needs a minute or more of additional energy after the observation of the completed rupture before an accurate estimate can be made. In this study, we propose a new method that can be computed on individual stations following cessation of observed rupture.

[4] An earthquake's dynamic rupture process is also characterized by E [*Boatwright and Choy*, 1986; *Venkataraman and Kanamori*, 2004]. While the seismic moment M_0 defines the work performed in an earthquake, E describes the strength of the event; information particularly useful in estimating the strong ground shaking and tsunami hazard [*Choy and Boatwright*, 1995]. In the case of earthquakes with high apparent stress drop, shaking can be over 10 times larger than expected given M_0 [*Choy and Kirby*, 2004]. For earthquakes in the shallow subduction megathrust, the rupture velocity V_R is greatly reduced, and hence little high-frequency shaking is observed [*Bilek and Lay*, 1999]. In such cases, E decreases considerably relative to M_0 and serves as a discriminant for slow rupturing "tsunami earthquakes" (TsE) [*Newman and Okal*, 1998]. It is this deficiency in high-frequency energy that led *Kanamori* [1972] to define TsEs as having much larger tsunami than expected given their magnitude.

[5] While both T_R and E are independently useful for assessing an earthquake's size, the combination of these is a powerful tsunami earthquake discriminant, because while M_0 scales with the cube of the T_R for most earthquakes [*Houston*, 2001], slow TsEs are both deficient in E and excessive in T_R. *Newman et al*. [2011] combined E and T_R^3 for the real-time discrimination of the 2010 Mentawai TsE. This method, while similar to the (E/M_0), does not require the accurate estimation of M_0, rendering it more useful for real-time evaluation.

2. Methods

[6] We calculate the radiated seismic energy at teleseismic stations (between 25° and 80°) following *Boatwright and Choy* [1986]. For these stations, we acquire the vertical component of velocity seismograms containing the *P*-wave group ($P + sP + pP$), and compute the cumulative radiated seismic

[1]School of Earth and Atmospheric Sciences, Georgia Institute of Technology, Atlanta, Georgia, USA.

Corresponding author: J. A. Convers, School of Earth and Atmospheric Sciences, Georgia Institute of Technology, 311 Ferst Drive, Atlanta, GA 30332, USA. (jconvers@gatech.edu)

0094-8276/13/10.1002/2013GL057664

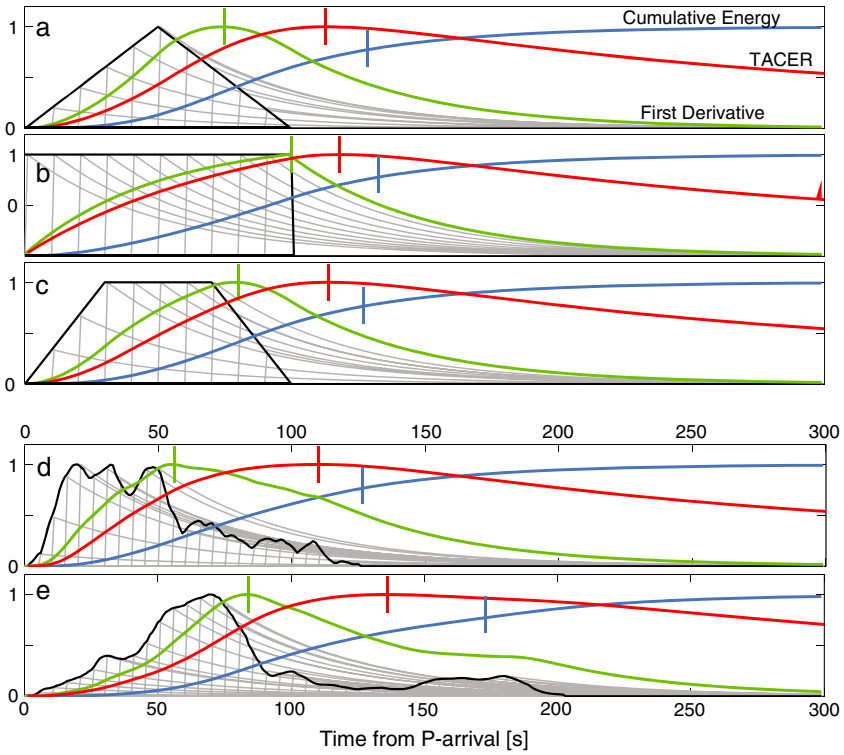

Figure 1. Source time functions (black) are shown along with their predicted energy distribution at a teleseismic station using a simple exponential decay mimicking scattering. The energy per time step (gray) is combined to show the cumulative energy release (blue), the first derivative of cumulative energy growth (green), and TACER (red). Three theoretical time histories for (a) triangular, (b) boxcar, and (c) trapezoidal functions and time histories for (d) the M_W 7.8 2010 Mentawai tsunami earthquake [*Newman et al*., 2011], and (e) the M_W 9.0 2011 Tohoku-Oki earthquake [*Hayes et al*., 2011].

energy flux in the frequency domain, according to the equation

$$\varepsilon^* = \frac{\rho\alpha}{\pi}\int_0^\infty |\omega\,\dot{u}|^2 e^{\omega t^*(\omega)} d\omega, \qquad (1)$$

where ρ and α are the density and *P*-wave velocity of the source region, $\dot{u}$ is the velocity of particle motion at the seismic station, and $t^*(\omega)$ is the globally averaged frequency-dependent attenuation factor [*Choy and Boatwright*, 1995]. To allow for direct corrections for frequency-dependent attenuation, energy calculations are performed in the frequency domain using incrementally growing time windows [*Convers and Newman*, 2011]. To calculate the seismic energy radiated from the source region, one must also correct for geometric spreading, partitioning of energy between *P* and *S* waves, and the orientation of the focal mechanism [*Boatwright and Choy*, 1986], or use an empirical average focal correction for real-time implementation [*Newman and Okal*, 1998]. However, source duration estimates require no geometric, focal, or energy partitioning corrections, as they each linearly scale the time history for any individual station-event pair. Because we routinely perform real-time and post-processed radiated energy calculations for these earthquakes, the energy results are included.

[7] To consider the performance of proposed and existing methods for numerically evaluating the rupture duration based on energy signals in teleseismic *P*-waves, we compare results based on simple synthetic and complex measured source-time functions. For each source-time function, we assume each second of rupture equates to an individual pulse of scaled energy whose individual pulses sum to the total radiated seismic energy (Figure 1). Each pulse exhibits a constant exponentially decaying tail representing the averaged scattered energy between source and receiver at teleseismic distances. The summation of pulses yields the cumulative energy growth as used in *Convers and Newman* [2011] for the determination of the crossover duration T_{XO}. For each triangular, boxcar, and trapezoidal synthetic energy source time functions (cases a, b, and c) and source-time functions for two complex ruptures (cases d and e), including the 2010 Mentawai tsunami earthquake [*Newman et al*., 2011], and the 2011 Tohoku-Oki earthquake [*Hayes et al*., 2011], we illustrate the behavior of T_{XO} and two proposed methods for identifying the termination of rupture (Figure 1).

[8] The maximum of the first derivative of the cumulative energy growth, representing the seismic energy release rate, is one potential rupture duration identifier that accurately identifies rupture duration in the case of a boxcar source (case b) (Figure 1). However, we find that peaks in the first-derivative energy tend to lag the peak moment-release, yet occur before rupture terminates in each of the synthetic triangle and trapezoid sources (cases a and c) and two test earthquakes (cases d and e). In large and prolonged ruptures with complex source-time functions, the process of identifying duration is not straightforward, since an examination based on the first derivative would become, in practice, a search for either a prominent decrease in the first derivative, or a search for a point where

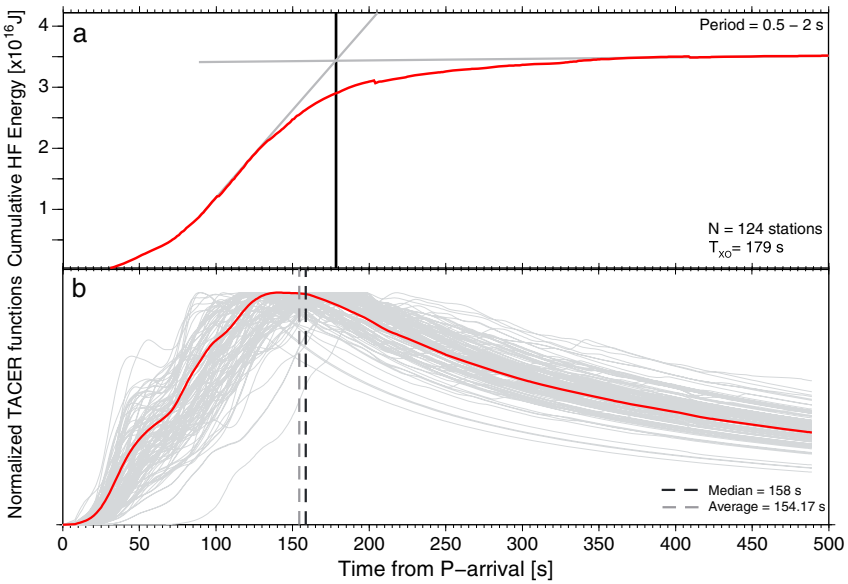

Figure 2. Duration estimates for the 2011 Tohoku-Oki M_W 9.0 earthquake. (a) The cumulative high-frequency energy is calculated from the average growth of 124 available broadband stations, yielding $T_{XO} = 179$ s. (b) The per station (gray) and median (red) TACER solutions are shown for this event. T_{TACER} represented as the median (black dashed line; = 158 s) or average (gray dashed line; = 154 s) is somewhat earlier than T_{XO}.

the first derivative falls to a certain value after a maximum, which again potentially becomes a subjective procedure.

[9] A second and preferred method for estimating earthquake rupture duration is an adaptation of the energy growth, called the time-averaged cumulative energy rate (TACER). With TACER, we attempt to minimize the effect of small jumps in the cumulative energy growth while minimizing edge effects associated with short-window energy calculations in the frequency domain. In its discrete form, TACER is

$$\mathrm{TACER}(t_n) = \frac{\sum_{i=1}^{n} \Delta E_i / \Delta t_i}{t_n}, \qquad (2)$$

where the result, a function of time t from the first P-arrival, is determined as the summation of the time derivatives of the cumulative high-frequency (0.5–2 Hz) energy. The rupture duration T_{TACER} is calculated at the maximum TACER value, which is also the local maximum in most cases. In every test case, T_{TACER} is longer than the first-derivative maximum and is closer to the T_R in cases where the source diminishes before ceasing (cases a, c, d, and e). While no one method is ideal in all situations, T_{TACER} is closer than T_{XO} and the first derivative duration to the theoretical rupture termination in the two cases where there is regular energy falloff (triangular and trapezoidal sources). In the two example long-duration earthquakes, T_{TACER} was similar but somewhat shorter than T_{XO}, which accurately estimated the rupture termination.

[10] One advantage that remains with T_{TACER} over T_{XO} is that TACER calculations can be routinely determined per-station, rather than from a stack of all waveforms as T_{XO} is normally done [*Convers and Newman*, 2011]. With the per-station solutions, we are able to evaluate per-event duration and energy ranges based on the variance of the collected data. Using these data, we can report the optimal median solution and the 75% range (see supporting information Table S1). This is chosen over a mean, since per-station solutions tend to include long tails with excessive duration due to later arriving reflected phases (e.g., *PcP*) or near-receiver signals that would otherwise bias the mean.

[11] Our data set covers the global catalog of earthquakes of moment magnitude $M_W \geq 7.0$ recorded at teleseismic distances since January 2000 and in real time from 2009, using a set of algorithms collectively called "*RTerg*" (http://geophysics.eas.gatech.edu/RTerg). The algorithms automatically calculated both the duration and value of seismic energy release in increasing time-windows at two different bandwidths (0.5–70 s for broadband energy "E" and 0.2–5 s for high-frequency energy "E_{hf}"). While broadband energy is used to calculate the total radiated energy (and energy magnitude, M_e), the high-frequency energy, which helps characterize strong shaking, is used to approximate rupture duration due to its ability to filter out later body-wave arrivals [*Convers and Newman*, 2011].

3. Results and Discussion

[12] The application of this method to real-time situations aids in the rapid assessment of earthquake rupture duration and total energy release. In Figure 2, we illustrate the application of T_{XO} and T_{TACER} for the recent 2011 Tohoku-Oki M_W 9.0 earthquake. Using the same 124 globally distributed stations for both methods, we found comparable results between T_{XO} and T_{TACER} ($T_{XO} = 179$ s, $T_{TACER} = 158$ s, 124–186 s 75% bounds), similar to other results of 150–160 s [*Ammon et al.*, 2011] and somewhat lower than ~200 s result from *Hayes* [2011]. Though there is no clear directivity effect in duration, due to its largely bilateral rupture, the seismic energy radiation was far stronger in the Western Hemisphere (see supplementary text and Figure S1). While directivity effects are not always apparent, in cases of long unilateral ruptures and good azimuthal station distribution, the per-station behavior of TACER may identify additional useful earthquake parameters in near-real time. We explore one case example for the M_W 8.1 2007 Solomon Islands

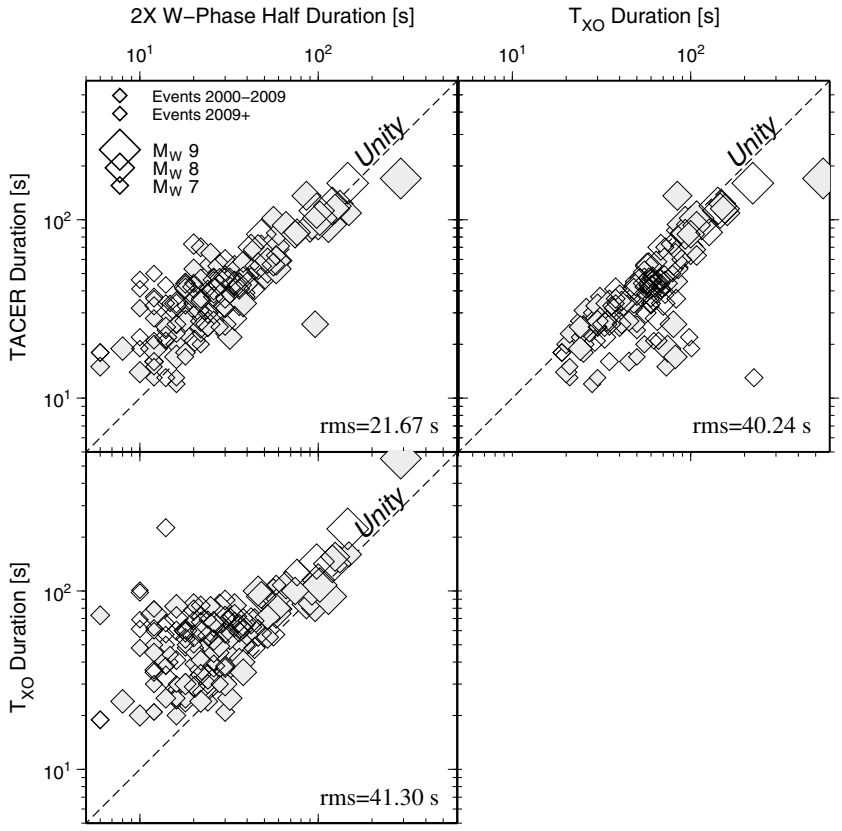

Figure 3. Comparison of the T_{TACER} with T_{XO} [*Convers and Newman*, 2011] and *W*-phase [*Duputel et al*., 2012] durations. The *W*-phase durations are reported as 2× the half duration of their catalogs. The rms differences for each comparison study are shown, and T_{XO} solutions are differentiated between retrospective (2000–2009) and real time (after 2009).

earthquake, in which near-ideal station spacing and long rupture allowed for a clear estimation of rupture propagation direction, rupture length, and approximate rupture velocity (see supplementary text and Figure S2). Attempts at several other well-known unilateral ruptures were less successful because of limited spatial resolution and rupture complexity.

[13] To test the robustness of median earthquake T_{TACER} results, we compare it to each of the duration estimates as calculated though the *W*-phase moment estimates [e.g., *Duputel et al*., 2012, 2013], and our solutions for T_{XO} [*Convers and Newman*, 2011] (Figure 2). For the first, duration is reported as 2× the half-duration reported in the catalog. While there is no definite method for estimating durations from any of these robust catalogs, we view the *W*-phase catalog to be most representative, as solutions are dependent on the long-period elastic signal due to the displacement field created across the entire rupture area of the earthquake. The solutions are differentiated between those that were determined retrospectively between 2000 and 2009 and those between 2009 and 2012 determined using automated real-time solutions. Though large scatter remains for individual T_R determinations, there is little large-scale bias between the solutions. In comparing rms residuals between methods, we find that T_{TACER} behaves comparably to T_R as determined by *W* phase (rms ~20 s) and performs about twice as well as T_{XO} (~40 s). A positive bias exists for T_{TACER} at small magnitudes (Figure 3). This lower bound bias, which is smaller than the one found with T_{XO}, likely comes from a combination of scattering within the earth and the temporal separation between the direct *P* and the depth phases, which is approximately 16 s at teleseismic distances for an earthquake at 40 km depth. For some larger earthquakes, half-durations which are based on regularly shaped moment release (e.g., triangular function in Figure 1a), will underestimate rupture duration as the methods best fit the largest moment release rather than the total slip over time.

[14] The TACER method was implemented into our real-time assessment tool, "*RTerg*", in early 2009. Using these results, we evaluated the performance of both median earthquake solutions and per-station solutions over time (Figure S3). Ninety percent (90%) of *median* solutions are within 10% of the final median result within 6 min. Similarly, 90% of the per-station solutions are within 20% of the final median result within 14 min. Thus, while individual TACER solutions may be reliable in some instances, more stations with good azimuthal coverage are preferable. Finally, we tested the effect azimuthal sampling had on the determination of median T_{TACER}, but found that no substantial biases existed between total station medians, and medians taken including 5°, 10°, or 15° local median solutions (Figure S4). Regardless, to provide more rapid and minimally biased solutions, one may consider similar spatial subsampling of available stations to avoid largely redundant data. For many earthquakes, tsunami arrives at the shore typically 30 min or more after the initial rupture due to the distance from the trench [e.g., *Fritz et al*., 2007].

[15] Because TACER reliably estimates durations in real time, it is useful for early earthquake information and potentially tsunami warning in the case of very large and tsunami earthquakes. While the energy methods are more problematic at distances less than 25° due to triplication effects, a recent

study by *Ebeling and Okal* [2012] suggests that energy calculations can be made much closer by applying a distance-based empirical correction that reduces the final energy calculation by up to an order of magnitude at distances less than 10°. Thus, the combination of such a correction with a systematic evaluation of near-field station duration estimates may yield an improved rapid near-field duration result.

[16] Some limitations beyond the geometric constraints remain. These come from the complexity of earthquake rupture, deep earthquakes, and the occurrence of overlapping waveforms from multiple earthquakes. For complex ruptures, such as the case of two strong patches with some delay, the energy release can be biased toward the first rupture patch, giving a shortened duration estimate. For deeper earthquakes, the depth phases are increasingly delayed, and depending on the orientation of the focal sphere, the delay may appear even larger than the direct *P*-arrival and may appear excessively long. For small earthquakes, the travel-time difference between the direct and depth phases becomes large relative to the rupture duration and can systematically overestimate rupture duration. Finally, when two or more earthquakes rupture within a few minutes time, their energy can be superimposed at teleseismic distances. Normally, this occurs when very large earthquakes have immediate aftershocks, but can also occur when a coincident event occurs elsewhere. Because of the contamination of energy, the later earthquakes are often ill determined, and spurious results are reported. Such cases are not surprising, and analysts should be aware of the possible scenario.

4. Conclusions

[17] Rupture duration is an important earthquake parameter that is generally obtained by modeling source-time functions or by visual and sometimes subjective examination of seismogram. We introduce the time-averaged cumulative energy rate (TACER) method which provides a rapid and robust estimation of rupture duration, which when combined with algorithms that routinely calculate earthquake energy in real time can be used for improved early earthquake information and tsunami warning [e.g., *Newman et al*., 2011]. The durations we obtain from TACER are comparable to those obtained by *W*-phase inversion and are an improvement over T_{XO}, as they show less overestimation for smaller earthquakes, and can be calculated for each recording station. Using the azimuthal variations in T_{TACER}, for earthquakes with long and unilateral rupture, it may be possible to provide early information about the geometry and extent of rupture from directivity effects.

[18] **Acknowledgments.** We thank Gavin Hayes for helping us gather the W-Phase half duration information for catalog comparison. Also, the efforts by Alexander Hutko, Harley M. Benz, and an anonymous reviewer were substantial and greatly improved the final manuscript.

[19] The Editor thanks Alexander Hutko, Harley M. Benz, and an anonymous reviewer for their assistance in evaluating this paper.

References

Ammon, C. J., T. Lay, H. Kanamori, and M. Cleveland (2011), A rupture model of the 2011 off the Pacific coast of Tohoku Earthquake, *Earth Planets Space*, *63*(7), 693–696.

Bilek, S. L., and T. Lay (1999), Rigidity variations with depth along interplate megathrust faults in subduction zones, *Nature*, *400*(6743), 443–446.

Boatwright, J., and G. L. Choy (1986), Teleseismic estimates of the energy radiated by shallow earthquakes, *J. Geophys. Res.*, *91*(B2), 2095–2112.

Choy, G. L., and J. L. Boatwright (1995), Global patterns of radiated seismic energy and apparent stress, *J. Geophys. Res.*, *100*(B9), 18,205–18,228.

Choy, G. L., and S. H. Kirby (2004), Apparent stress, fault maturity and seismic hazard for normal-fault earthquakes at subduction zones, *Geophys. J. Int.*, *159*(3), 991–1012.

Convers, J. A., and A. V. Newman (2011), Global evaluation of large earthquake energy from 1997 through mid-2010, *J. Geophys. Res.*, *116*, B08304, doi:10.1029/2010JB007928.

Duputel, Z., L. Rivera, H. Kanamori, and G. Hayes (2012), W phase source inversion for moderate to large earthquakes (1990–2010), *Geophys. J. Int.*, *189*(2), 1125–1147.

Duputel, Z., V. C. Tsai, L. Rivera, and H. Kanamori (2013), Using centroid time-delays to characterize source durations and identify earthquakes with unique characteristics, *Earth Planet. Sci. Lett.*, *374*, 92–100.

Ebeling, C. W., and E. A. Okal (2012), An extension of the E/M_0 tsunami earthquake discriminant θ to regional distances, *Geophys. J. Int.*, *190*(3), 1640–1656.

Fritz, H. M., et al. (2007), Extreme runup from the 17 July 2006 Java tsunami, *Geophys. Res. Lett.*, *34*, L12602, doi:10.1029/2007GL029404.

Hara, T. (2007), Measurement of the duration of high-frequency energy radiation and its application to determination of the magnitudes of large shallow earthquakes, *Earth Planets Space*, *59*(4), 227–231.

Hayes, G. P. (2011), Rapid source characterization of the 2011 *Mw* 9.0 off the Pacific coast of Tohoku Earthquake, *Earth Planets Space*, *63*(7), 529–534.

Hayes, G. P., P. S. Earle, H. M. Benz, D. J. Wald, R. W. Briggs, and U. N. E. R. Team (2011), 88 Hours: The U.S. Geological Survey National Earthquake Information Center Response to the 11 March 2011 *Mw* 9.0 Tohoku Earthquake, *Seismol. Res. Lett.*, *82*(4), 481–493.

Houston, H. (2001), Influence of depth, focal mechanism, and tectonic setting on the shape and duration of earthquake source time functions, *J. Geophys. Res.*, *106*(B6), 11,137–11,150.

Kanamori, H. (1972), Mechanism of tsunami earthquakes, *Phys Earth Planet. In.*, *6*, 346–359.

Lomax, A. (2005), Rapid estimation of rupture extent for large earthquakes: Application to the 2004, M9 Sumatra-Andaman mega-thrust, *Geophys. Res. Lett.*, *32*, L10314, doi:10.1029/2005GL022437.

Newman, A. V., and E. A. Okal (1998), Teleseismic estimates of radiated seismic energy: The E/M_0 discriminant for tsunami earthquakes, *J. Geophys. Res.*, *103*(B11), 26,885–26,898.

Newman, A. V., G. Hayes, Y. Wei, and J. A. Convers (2011), The 25 October 2010 Mentawai tsunami earthquake, from real-time discriminants, finite-fault rupture, and tsunami excitation, *Geophys. Res. Lett.*, *38*, L05302, doi:10.1029/2010GL046498.

Venkataraman, A., and H. Kanamori (2004), Observational constraints on the fracture energy of subduction zone earthquakes, *J. Geophys. Res.*, *109*, B05302, doi:10.1029/2003JB002549.